Journal of Applied Polymer Science

Silicone Membranes to Inhibit Water Uptake into Thermoset Polyurethane Shape-Memory Polymer Conductive Composites

Ya-Jen Yu,[1] Stephen Infanger,[1] Melissa A. Grunlan,[1,2] Duncan J. Maitland[1]

[1]Department of Biomedical Engineering, Texas A & M University, College Station, Texas 77843

[2]Department of Materials Science and Engineering, Texas A & M University, College Station, Texas 77843

Correspondence to: D. J. Maitland (E-mail: djmaitland@tamu.edu)

ABSTRACT: Electroactive shape memory polymer (SMP) composites capable of shape actuation via resistive heating are of interest for various biomedical applications. However, water uptake into SMPs will produce a depression of the glass transition temperature (T_g) resulting in shape recovery *in vivo*. While water actuated shape recovery may be useful, it is foreseen to be undesirable during early periods of surgical placement into the body. Silicone membranes have been previously reported to prevent release of conductive filler from an electroactive polymer composite *in vivo*. In this study, a silicone membrane was used to inhibit water uptake into a thermoset SMP composite containing conductive filler. Thermoset polyurethane SMPs were loaded with either 5 wt % carbon black or 5 wt % carbon nanotubes, and subsequently coated with either an Al_2O_3- or silica-filled silicone membrane. It was observed that the silicone membranes, particularly the silica-filled membrane, reduced the rate of water absorption (37°C) and subsequent T_g depression versus uncoated composites. In turn, this led to a reduction in the rate of recovery of the permanent shape when exposed to water at 37°C. © 2014 Wiley Periodicals, Inc. J. Appl. Polym. Sci. **2015**, *132*, 41226.

KEYWORDS: biomedical applications; conducting polymers; thermosets; polyurethanes

Received 10 April 2014; accepted 26 June 2014

DOI: 10.1002/app.41226

INTRODUCTION

Thermosensitive shape memory polymers (SMPs) are one type of smart material.[1] The permanent geometry can be sequentially deformed into a temporary geometry when heated above the transition temperature (T_{trans}), the secondary geometry fixed by cooling below T_{trans} and the original shape recovered upon heating above T_{trans}. Conductive fillers, such as carbon black (CB),[2] nanotubes (CNT),[3] and carbon nanofibers[4] have been incorporated into thermoplastic SMP systems to actuate the shape recovery via voltage-induced current rather than environmental heat.

The addition of fillers into the SMP matrix can increase the recovery stress as well as improve other mechanical properties such as modulus.[5] While thermoset SMP systems have the potential to achieve robust mechanical properties, few studies have been focused on these because of synthetic and processing limitations.[6,7] As a result, thermoset SMP composites have been largely limited to styrene-based systems with conductive carbon filler,[8] epoxy-based systems reinforced with SiC,[9] and acrylate-based systems with magnetic Fe_3O_4 particles.[10]

Polyurethane (PU) SMPs have drawn significant attention for a broad range of applications.[11,12] While the vast majority are thermoplastics, thermoset PU SMP systems having high recovery strains and stresses have been reported with potential use for biomedical applications.[13] In addition, we have reported ultra-low density thermoset PU SMP foams that undergo high volumes changes upon recovery from compressive strain and thus may have utility as embolic sponges to treat aneurysms.[14,15]

The effect of water uptake on shape memory behavior and physical properties of thermoplastic PU SMPs has been reported.[16] It was shown that moisture absorption led to a decrease in T_g due to weakening of the hydrogen bonding between N—H and C=O groups. Thus, the absorbed water acted as a plasticizer.[17] Due to the decreased T_g (i.e., decreased T_{trans}), a loss of shape fixity was also observed and specimens exhibited shape recovery upon immersion in 37°C water. In the case of conductive SMP composites, release of conductive fillers *in vivo* remains yet another substantial concern.[18] For this reason, various membranes such as parylene C,[19,20] polytetrafluoro ethylene,[21] and silicones[22,23] have been proposed as protective barrier coatings. Thus, the utility of thermoset PU SMP conductive composites in biomedical applications would be enhanced if the water absorption and potential release of filler could be controlled. However, the use of such a membrane to impede water absorption into an SMP conductive composite has not yet been explored.

Herein, thermoset PU SMP conductive composites were prepared with CB and CNT fillers and coated with a silicone membrane to hinder water absorption. In terms of biomedical applications, the extreme hydrophobicity,[24,25] as well as biocompatibility, biodurability, and thermal and oxidative stability[26–28] make silicones an ideal candidate. Since silicones are typically reinforced,[28] both an Al_2O_3- and silica-filled silicones were evaluated in this study. The silicone-coated SMP composites were subjected to conditioning in water (37°C) and the resulting water uptake as well as rate and extent of the T_g depression were compared to uncoated controls. In addition, shape recovery (i.e., diminished shape fixity) of coated- and uncoated-SMPs in a 37°C aqueous environment was compared.

EXPERIMENTAL

Materials

Trifunctional polyol triethanolamine (TEA; Sigma Aldrich, 99%), tetrafunctional polyol *N,N,N′,N′*-tetrakis (2-hydroxypropyl) ethylenediamine (HPED; TCI America, 98%), and hexamethylene diisocyanate (HDI; TCI America, 98%) were used as received. CB (ENASCO® 250; primary particle size ~40 nm, density 0.17 g cm^{-3} per manufacturer's specification) was obtained from TIMCAL Graphite and Carbon. Multiwall CNTs (dimensions 110–170 nm × 5–9 μm, density 1.7 g cm^{-3} per manufacturer's specification) were obtained from Sigma Aldrich. Al_2O_3-filled silicone (SYLGARD® Q3–3600) was obtained from Dow Corning. Per manufacturer's specifications, Q3–3600 comprises: *Part A*: methyltrimethoxysilane treated aluminum oxide (70–90%), dimethyl siloxane (15–35%), methylvinyl siloxane (1–5%), and methyl alcohol (<0.01%); *Part B*: methyltrimethoxysilane treated aluminum oxide (70–90%), dimethyl siloxane (15–35%), methylhydrogen siloxane (3–7%), carbon black (<1%), and methyl alcohol (<0.01%). Medical-grade silica-filled silicone (MED-1137) was obtained from NuSil Technology. Per manufacturer's specifications, MED-1137 comprises: *α,ω-bis*(Si-OH)PDMS, silica (11–21%), methyltriacetoxysilane (<5%), ethyltriacetoxysilane (<5%), and trace amounts of acetic acid. Hexane (95%, anhydrous) was obtained from Sigma Aldrich. Polypropylene molds were obtained from TAP Plastics.

Preparation of SMP Composites

The PU thermoset matrices were prepared from the mole ratio of TEA : HPED : HDI of 0.133 : 0.4 : 1. **CB5** (i.e., SMP composite containing 5 wt % CB) and **CNT5** (i.e., SMP composite containing 5 wt % CNT) were prepared as follows: CB and CNTs were initially dispersed in the HPED at 5 wt % using a FlackTek 150 DAC speed mixer (3400 rpm, 30 s). Next, the HPED/carbon filler dispersions were likewise sequentially blended with TEA and HDI. The final mixtures (62 mL) were cast into polypropylene molds (9 × 7 × 3 cm) and then heat-treated (120°C oven, 60 min) to initiate polymerization. The resulting specimens were removed from the molds and polished to a thickness of ~1 mm by computer numerical control (Roland MDX-540). A neat SMP control (**SMP**) was prepared as above but without introduction of carbon filler.

Prior to coating with silicone, the SMP composites were cut into 25 × 3 × 1 mm specimens using a CO_2 laser cutter (Gravograph 40 W LS100). To permit dip coating, the specimens were suspended from one end of a polypropylene rod with a small amount of epoxy glue. The other end of the rod was inserted into a hole of a custom-made polycarbonate circular plate that could support up to ten rods. The top side of the circular plate was attached to a motion controller (Newport ESP3000). Al_2O_3-filled silicone was prepared by mixing Parts A and B (50 : 50 wt %) with the high speed mixer (3400 rpm, 30 s). The silica-filled silicone was prepared by dissolving in hexane (45 : 55 wt %) overnight and stirring with a Teflon covered magnetic stir bar. Specimens were dip coated into the designated silicone by dipping at a rate of 2 mm min^{-1} (into the silicone), holding for 2 min, and finally removing at a rate of 2 mm min^{-1}; then, the entire process was repeated. The resulting Al_2O_3-filled silicone-coated specimens (**CB5/silicone-$_{Al2O3}$** and **CNT5/silicone-$_{Al2O3}$**) were cured in an oven (90°C) for 2 h. The resulting silica-filled silicone-coated specimens (**CB5/silicone-$_{silica}$** and **CNT5/silicone-$_{silica}$**) were sequentially cured at room temperature (RT) for 1 h and at 70°C for 6 h. After curing, the specimens were removed from the rods and epoxy glue was carefully applied to seal the end of the specimens.

Free-standing silicone membranes (**silicone-$_{Al2O3}$** and **silicone-$_{silica}$**) were prepared by casting the aforementioned Al_2O_3-filled silicone mixture and silica-filled silicone solution (10 mL) into molds (9 × 7 × 3 cm) and curing as above.

Gross Appearance

Gross images of all specimens were obtained with a ProgRes digital camera (Jenoptik) attached to Leica MZ16 stereomicroscope.

Resistivity

The electrical resistivity of **CB5 and CNT5** (i.e., uncoated SMP composites) were compared to that of **SMP** as follows: Rectangular specimens (30 × 5 × 2 mm) were machined using Gravograph 40 W LS100 CO_2 laser machining instrument. Resistivity was measured with a four-point probe SP4 (Signatone) apparatus equipped with an Agilent 34401A multimeter, Agilent 34420A micro-ohm meter, and Agilent E3632A DC power supply.

Scanning Electron Microscopy (SEM)

SEM was used to evaluate the morphological features of the specimens as well as silicone membrane thickness. Uncoated (i.e., **SMP**, **CB5**, **CNT5**) and **silicone-coated** (i.e., **CB5/silicone-$_{Al2O3}$**, **CNT5/silicone-$_{Al2O3}$**, **CB5/silicone-$_{silica}$**, and **CNT5/silicone-$_{silica}$**) specimens were dried under vacuum at 90°C for 12 h. Cross sections were prepared by cutting with a clean razor blade. Surface and cross sectional specimens were subjected to gold sputter coating (Ted Pella 6002) and viewed with a JEOL Neoscope JCM-5000 SEM at an accelerating voltage of 15 kV. The thicknesses of the Al_2O_3-filled silicone and silica-filled silicone membranes coated on SMP composites were obtained from cross sectional SEM images. For a given coated composite, five specimens were cut in half with a clean razor blade. The resulting 10 cross sectional surfaces were each subjected to SEM and thickness measured at three different designate areas.

Thermal Gravimetric Analysis (TGA)

TGA (TA Instruments Q50) was performed on **SMP**, **CB5**, **CNT5**, **silicone-$_{Al2O3}$**, and **silicone-$_{silica}$**. Specimens (~10 mg)

were placed in platinum pans and heated under N_2 at a flow rate of 60 cm^3 min^{-1}. The sample weight was recorded while the temperature was increased 10°C min^{-1} from 30 and 800°C.

Contact Angle

The static contact angle (θ_{static}) of distilled/DI water droplets at the surface–air interface were measured by a CAM200 (KSV Instruments) goniometer equipped with an autodispenser, video camera, and drop-shape analysis software. A sessile drop of water (5 μL) was measured at 15 s following deposition via needle onto the specimen surface. For **SMP**, **CB5**, **CNT5**, **silicone-$_{Al2O3}$**, and **silicone-$_{silica}$**, the reported values are an average of three measurements taken on different areas of the same specimen.

Water Absorption

The water uptake by **SMP**, **CB5**, **CNT5**, **silicone-$_{Al2O3}$**, and **silicone-$_{silica}$** was measured gravimetrically. Specimens (5 × 5 × 1 mm) were weighed (W_i) and then immersed into 37°C deionized (DI) water bath for 0.5, 2, 6, 24, 48, 96, and 192 h. At a designated time point, each specimen was removed from the water bath, blotted with a Kim Wipe and immediately weighed (W_f). Water absorption was quantified in terms of wt ratio of water, defined as:

$$\text{weight ratio water } (\%) = \left[\frac{W_f - W_i}{W_f}\right] \times 100 \quad (1)$$

For each specimen type, five measurements were completed.

Differential Scanning Calorimetry

T_g was determined via differential scanning calorimetry (DSC, TA Instruments Q200). First, T_g was monitored as a function of conditioning time in a 37°C deionized (DI) water bath. At designated time points (0.5, 2, 6, 24, 48, 96, and 192 h), specimens of **SMP**, **CB5**, **CNT5**, **CB5/silicone-$_{Al2O3}$**, **CNT5/silicone-$_{Al2O3}$**, **CB5/silicone-$_{silica}$**, and **CNT5/silicone-$_{silica}$** were collected, placed in hermitically sealed pans with a pin-hole punch through the top lid (for moisture evaporation) and heated from −40 to 150°C at 10°C min^{-1}. Second, specimens conditioned for 192 h in a 37°C DI water bath were subjected to cyclic DSC experiments and T_g recovery measured. Specimens likewise placed into DSC pans and sequentially heated (10°C min^{-1}) from −40°C to a specified temperature, held isothermally for 2 min, cooled to −40°C, and held isothermally for 2 min. A given specimens was subjected to seven consecutive heating cycles to 70, 90, 110, 130, 150, 170, and 190°C, with each subsequent cycle employing the next highest temperature in the series.

Peel Test

The peel strength of the silicone membranes coated onto the SMP composites was measured with a pull-off adhesion tester (DeFelsko PosiTest AT). Silicone-coated composites (**CB5/silicone-$_{Al2O3}$**, **CNT5/silicone-$_{Al2O3}$**, **CB5/silicone-$_{silica}$**, and **CNT5/silicone-$_{silica}$**) (9 × 7 × 1 cm) were placed inside a mold (9 × 7 × 3 cm). Next, the aforementioned Al_2O_3-filled silicone compound and silica-filled silicone solution (10 mL) were poured on top of the designated specimens residing in the molds. Five aluminum dollies (circular base, 10 mm diameter) were immediately set onto the uncured silicone layer of each specimen. Finally, the silicones were cured (so as to affix the dollies to the specimen) using the designated conditions previously described. The peel strength was measured before and immediately after soaking the each of the final test specimens (i.e., coated composite bearing five affixed dollies) in a 37°C DI water bath for 192 h. A cylindrical actuator connected to a hydraulic pump was used to produce a pulling force until the dolly separated from the specimen. Reported results are based on the average of the five tests conducted on a single specimen.

Shape Recovery

Specimens (25 × 3 × 1 mm) of **SMP**, **CB5**, **CNT5**, **CB5/silicone-$_{Al2O3}$**, **CNT5/silicone-$_{Al2O3}$**, **CB5/silicone-$_{silica}$**, and **CNT5/silicone-$_{silica}$** were heated to 110°C ($T > T_g$) and then immediately deformed into a temporary U-shape to approach an initial bending angle (θ_i) of 175–180°. The temporary shape was then fixed by equilibrating the specimens at RT ($T < T_g$). Next, the specimens were immersed in a 37°C DI water bath for 0.5, 2, 6, 24, 48, 96, and 192 h to measure the recovery of the original, permanent shape. The recovery angle (θ_r) images were recorded by a ProgRes digital camera (Jenoptik) attached to Leica MZ16 stereomicroscope. The shape recovery is expressed as:

$$\%\ \text{Recovery} = \left[\frac{\theta_i - \theta_r}{\theta_i}\right] \times 100 \quad (2)$$

RESULTS AND DISCUSSION

Resistivity and SEM

The gross appearance of the neat PU thermoset SMP, composites and silicone-coated composites are shown in Figure 1(a). While the presence of Al_2O_3 filler in the silicone renders it white and opaque, the silica-filled silicone is transparent. Resistivity measurements showed that **SMP** was insulating (10^{12} Ω cm) whereas **CB5** (10^3 Ω cm) and **CNT5** (10^2 Ω cm) were semiconducting. The resistivity of the composites is attributed to the formation of a percolating network of carbon filler.[29] SEM images of **CB5** [Figure 1(b)] and **CNT5** [Figure 1(c)] reveal the presence of CB and CNT, respectively. Representative cross sectional images of silicone-coated composites specimens are shown in Figure 1(d,e). Due to the nature of the dip coating process, the silicone membrane formed an oval surface over the rectangular SMP composite. The surface and cross sectional features are unique to the Al_2O_3-filled silicone coating [Figure 1(f,h)] and silica-filled silicone membranes [Figure 1(e,i)]. Notably, the higher level of filler for the Al_2O_3-filled silicone is quite apparent.

The thicknesses of the silicone membranes coated on top of the SMP composites are reported in Table I. Due to the resultant oval geometry, thickness was determined from measurements at three distinct regions (per Table I). The thickest portion of the membrane (representing the longest dimension of the specimen) was ~680 and ~530 μm for Al_2O_3-filled and silica-filled silicone, respectively. Perpendicular to this, membrane thickness was ~280 and ~220 μm, respectively. Finally, the thinnest membrane dimensions were found adjacent to the corner of the enclosed rectangular composite specimen. Here, the dimensions were ~65 and ~110 μm for Al_2O_3-filled and silica-filled

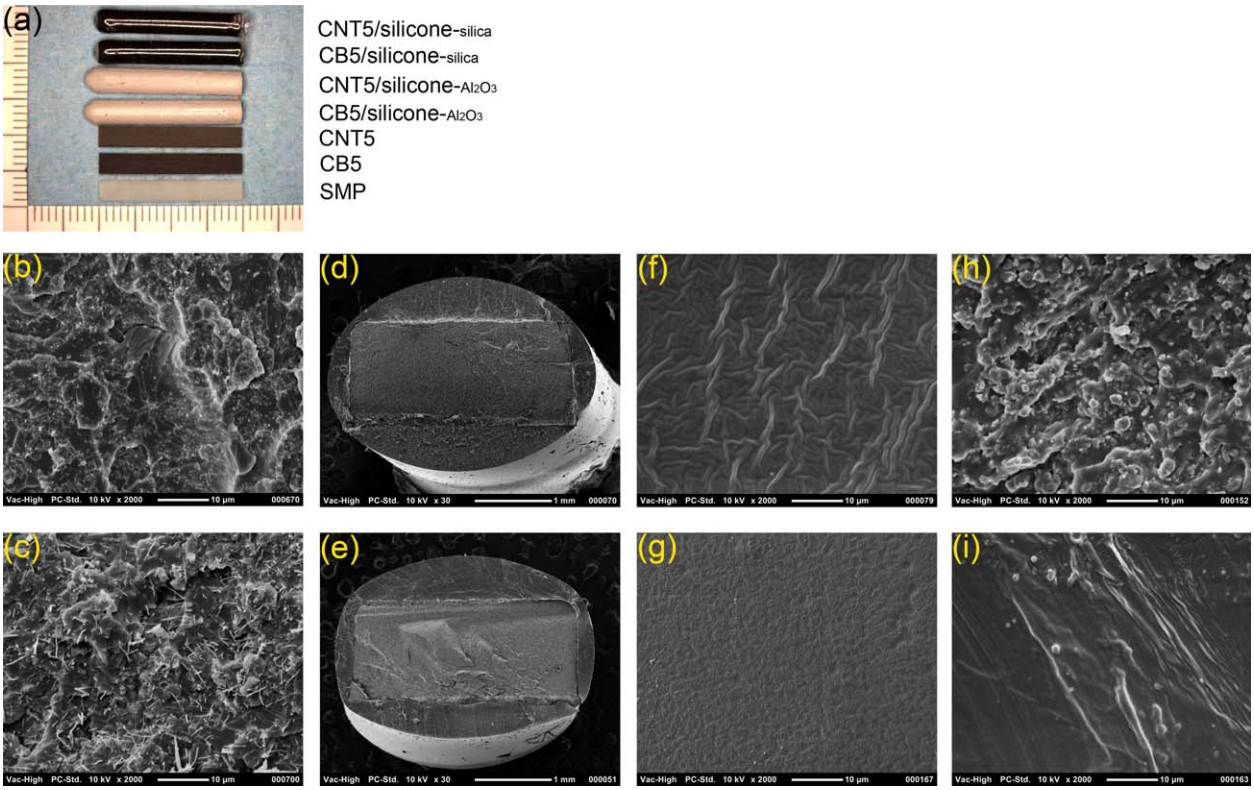

Figure 1. (a) Gross images of specimens (bottom to top): **SMP** (i.e., neat SMP); **CB5** and **CNT5** (i.e., SMP composite loaded with 5 wt % CB and CNT, respectively); **CB5/silicone-$_{Al2O3}$**, **CNT5/silicone-$_{Al2O3}$**, **CB5/silicone-$_{silica}$**, and **CNT5/silicone-$_{silica}$**) (i.e., silicone-coated composites). SEM images of (b) **CB5** cross section, (c) **CNT5** cross section, (d) **CB5/silicone-$_{Al2O3}$** cross section, (e) **CB5/silicone-$_{silica}$** cross section, (f) **silicone-$_{Al2O3}$** surface, (g) **silicone-$_{silica}$** surface, (h) **silicone-$_{Al2O3}$** cross section, (i) **silicone-$_{silica}$** cross section. [Color figure can be viewed in the online issue, which is available at wileyonlinelibrary.com.]

silicone, respectively. Thickness variations at different locations as well as differences between silicone membrane types may be attributed to the differences in competing forces (e.g., surface tension, evaporation, and capillary forces) associate with the dip coating process.[30]

TGA

Thermal decomposition of the neat SMP (**SMP**) began at ~260°C and produced an anticipated negligible char (Figure 2). Because of the inclusion of thermally stable filler,[31] the decomposition of **CB5** and **CNT5** was slightly increased versus that of **SMP**. The presence of ~5 wt % char for **CB5** and **CNT5** confirms the incorporation of 5 wt % of CB and CNT, respectively, into the SMP matrix. The observed high thermal stability of the silicone membranes (**silicone-$_{Al2O3}$** and **silicone-$_{silica}$**) is typical of that of cured silicone networks.[32] The presence of 70 and 20% char for **silicone-$_{Al2O3}$** and **silicone-$_{silica}$**, respectively, is consistent with their known quantities of Al_2O_3 and silica.

Table I. Sample Geometries

	Maximum thickness		
	Side A (μm)	Side B (μm)	Corner (μm)
CB5/Silicone-Al_2O_3[a]	687 ± 54	285 ± 38	64 ± 39
CNT5/Silicone-Al_2O_3[b]	675 ± 38	280 ± 29	68 ± 28
CB5/Silicone-silica[c]	534 ± 37	225 ± 26	108 ± 35
CNT5/Silicone-silica[d]	526 ± 49	216 ± 15	116 ± 43

[a] **CB5** coated with Al_2O_3-filled silicone.
[b] **CNT5** coated with Al_2O_3-filled silicone.
[c] **CB5** coated with silica-filled silicone.
[d] **CNT5** coated with silica-filled silicone.

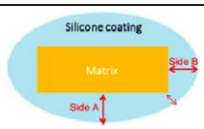

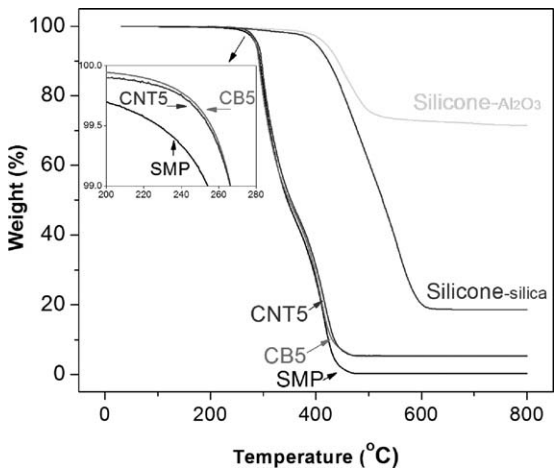

Figure 2. TGA of **SMP** (i.e., neat SMP); **CB5** and **CNT5** (i.e., SMP composite loaded with 5 wt % CB and CNT, respectively); **silicone-$_{Al2O3}$** and **silicone-$_{silica}$** (i.e., silicone membrane only).

Table II. Contact Angles

SMP θ_{static} (°)	CB5 θ_{static} (°)	CNT5 θ_{static} (°)	Silicone -Al_2O_3 θ_{static} (°)	Silicone-silica θ_{static} (°)
78.7 ± 2.8	117.3 ± 6.4	135.4 ± 12.8	121.7 ± 3.2	116.8 ± 1.8

Contact Angle Analysis

Contact angle analysis was used to assess wettability (Table II). Generally, a hydrophobic surface is characterized by $\theta_{static} \geq 90°$.[33] The neat PU thermoset SMP (**SMP**) exhibited a fairly hydrophilic surface ($\theta_{static} = \sim 79°$). Due to the addition of hydrophobic fillers, **CB5** and **CNT5**, were notably more hydrophobic ($\theta_{static} = \sim 117°$ and $\sim 135°$, respectively). The somewhat greater hydrophobicity of **CNT5** may be associated with the surface roughening effect associated with CNT fillers.[34,35] As expected for crosslinked silicones,[24,25] the membranes (**silicone-$_{Al2O3}$** and **silicone-$_{silica}$**) were very hydrophobic, exhibiting θ_{static} values of $\sim 122°$ and $\sim 117°$, respectively.

Water Absorption

Due to its hydrophilicity, the neat PU thermoset SMP (**SMP**) exhibited substantial water absorption, even after only 0.5 h exposure to DI water (37°C) (Figure 3). Between 0.5 and 192 h of exposure, the wt % ratio of water continued to increase considerably from ~1.7 to 5%. In the case of uncoated composites **CB5** and **CNT5**, due to the presence of the hydrophobic carbon fillers, the uptake of water was somewhat diminished relative to **SMP**. At all time points, the wt % ratio of water for **CB5** and **CNT5** were similar to one another and reached a maximum value of ~3.5% at 192 h. Due to their appreciable hydrophobicity, both **silicone-$_{Al2O3}$** and **silicone-$_{silica}$** membranes exhibited a lack of measurable water uptake even after 192 h.

Different Scanning Calorimetry

For the neat SMP, composites and silicone-coated composites, the depression of the T_g (of the thermosett PU SMP) was determined as a function of conditioning time in a 37°C water bath (Figure 4). For all specimen types, the T_g was ~71°C prior to conditioning. Due to the plasticizing effect of the absorbed water, the T_g of the neat SMP (**SMP**) decreased substantially from ~71 to ~60°C during the first 6 h of exposure. **CNB** and **CNB** showed only a slight lessening of the T_g depression during this period. In contrast, due to the presence of a hydrophobic silicone membrane, **CB5/silicone-$_{Al2O3}$**, **CNT5/silicone-$_{Al2O3}$**, **CB5/silicone-$_{silica}$**, and **CNT5/silicone-$_{silica}$** exhibited a much smaller change in T_g. Notably, T_g depression was the most diminished for composites coated with the silica-filled silicone. Thus, while water absorption could not be detected gravimetrically (Figure 3), a small amount of water is able to diffuse through the silicone membranes. The superior resistance of the silica-filled silicone may be attributed to its lower filler content versus the Al_2O_3-filled silicone. Upon continued conditioning, the T_g values of all specimens continued to decrease. However,

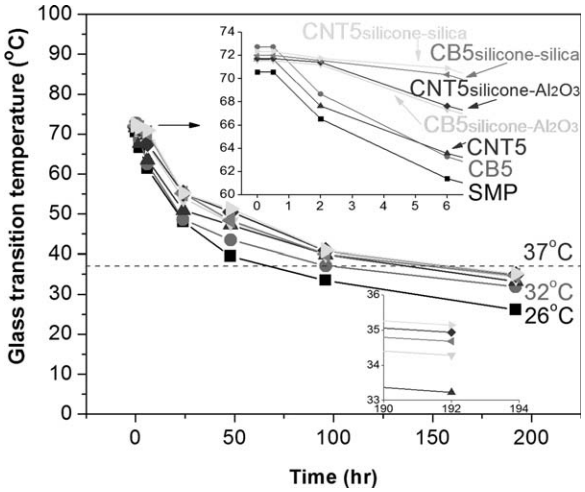

Figure 4. T_g vs. immersion time in a 37°C water bath for **SMP** (i.e., neat SMP); **CB5** and **CNT5** (i.e., SMP composite loaded with 5 wt % CB and CNT, respectively); and **CB5/silicone-$_{Al2O3}$**, **CNT5/silicone-$_{Al2O3}$**, **CB5/silicone-$_{silica}$**, and **CNT5/silicone-$_{silica}$** (i.e., composites coated with silicone membrane). ($T = 37$°C marked with dash line).

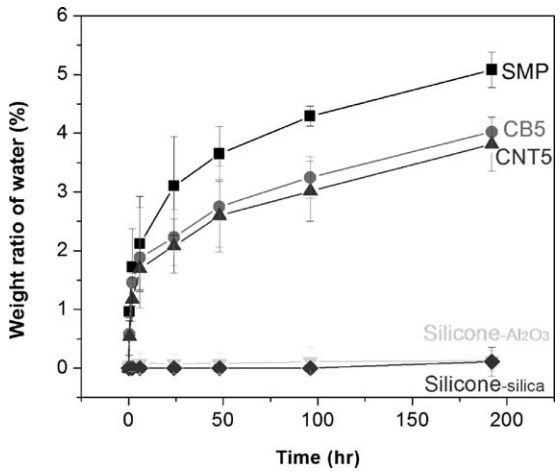

Figure 3. Weight % ratio of water (37°C) for **SMP** (i.e., neat SMP); **CB5** and **CNT5** (i.e., SMP composite loaded with 5 wt % CB and CNT, respectively); **silicone-$_{Al2O3}$** and **silicone-$_{silica}$** (i.e., silicone membrane only).

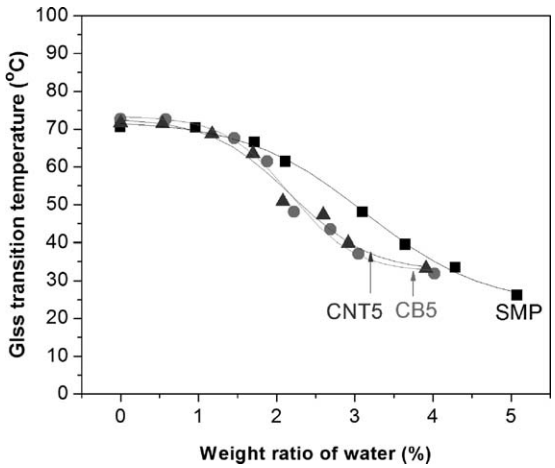

Figure 5. T_g as a function of weight ratio of water.

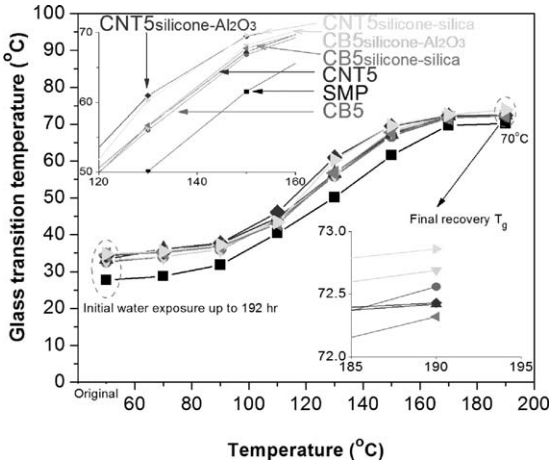

Figure 6. Recovery of T_g as a function of thermal cycling.

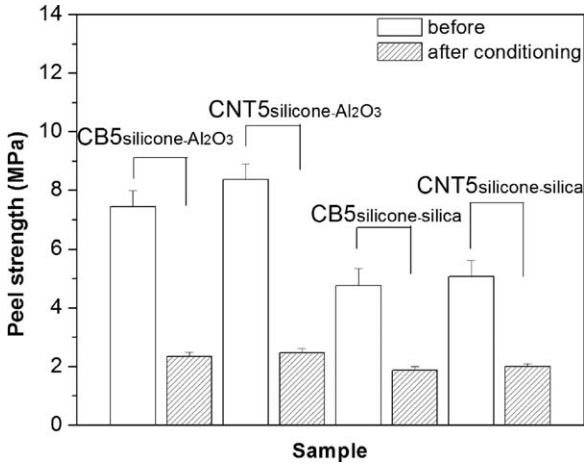

Figure 7. Peel strength of silicone membrane to **CB5** and **CNT5** composites before and after condition in a 37°C water bath for 192 h.

the silicone membrane delayed the depression of T_g to a value of 37°C or lower versus that of uncoated composites.

Based on data reported in Figures 3 and 4, T_g was plotted as a function of weight ratio of water for **SMP**, **CB5,** and **CNT5** (Figure 5). Since water uptake could not be determined for silicone-coated composites, these were not likewise analyzed. For **SMP**, a marked decrease in T_g occurs between 2 and 4% weight ratio of the water. Notably, for **CB5** and **CNT**, the decrease of T_g values with similar weight ratios of water is more substantial. Yang et al.[2] previously demonstrated that, when the water content of the system is sufficiently high, carbon fillers tend to lower the T_g value of a thermoplastic PU SMP versus the unfilled SMP.

In a previous study, Yang et al.[36] demonstrated that thermal cycling of a thermoplastic PU SMP previously conditioned in water can produce a recovery of the T_g due to dehydration. Thus, specimens previously conditioned in water for 192 h were immediately subjected to seven consecutive heating cycles in the order of 70, 90, 110, 130, 150, 170, and 190°C (Figure 6). These temperatures are below that shown to induce thermal decomposition (Figure 2). When cycled to 70 and 90°C, there was only a small increase in T_g values. However, T_g values substantially increased when cycled to 110, 130, and 150°C. This is attributed to effective drying (i.e., water evaporation) of the specimens. When cycled to 170°C, there was only a small increase in T_g values, indicating that specimens were already appreciably dehydrated. Finally, in the final heating cycle to 190°C, T_g values remained essentially unchanged, indicating that they were fully dehydrated. These final values are similar to their initital T_g values prior to conditioning (Figure 4).

Peel Test

Peel tests were conducted to measure the peel strength of silicone membranes to the underlying composites before and after conditioning in a 37°C water bath for 192 h (Figure 7). Prior to conditioning, peel strength was appreciably greater for the composites coated with the Al_2O_3-filled silicone versus the silica-filled silicone. However, after conditioning, the peel strength was only slightly higher for the Al_2O_3-filled silicone-coated composites. As noted, while water uptake cannot be measured gravimetrically for silicone-coated composites (Figure 3), the depression of T_g at 192 h (Figure 4) demonstrates that water is able to slowly diffuse through the membrane and weaken bonding but without inducing delamination.

Shape Recovery

The ability of specimens to retain their temporary fixed shape was measured in a percent recovery as a function of time conditioned in 37°C water (Table III). Shape recovery is predicted to

Table III. Shape Recovery Ratios

	Shape recovery ratio							
	0 h (%)	0.5 h (%)	2 h (%)	6 h (%)	24 h (%)	48 h (%)	96 h (%)	192 h (%)
SMP	0	3.6	7.1	12	44.6	89.2	99.0	100
CB5	0	0.8	1.9	9.4	37.8	82.6	98.2	100
CNT5	0	0.4	1.6	7.3	21.2	72.9	90.0	100
CB5/silicone-Al_2O_3	0	0.1	1.6	7.6	29.8	71.3	92.6	100
CNT5/silicone-Al_2O_3	0	0	1.0	5.7	19.6	67.6	87.2	100
CB5/silicone-silica	0	0	1.3	6.5	25.3	66.0	91.4	100
CNT5/silicone-silica	0	0	0.8	4.3	17.4	64.6	86.5	100

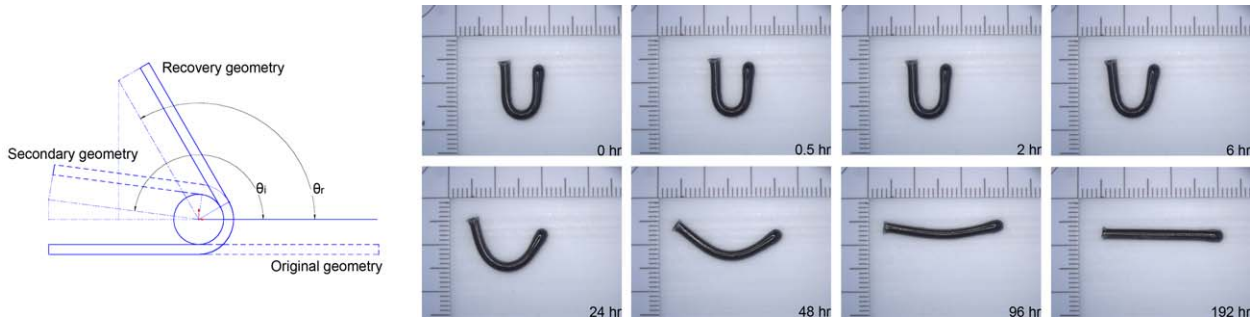

Figure 8. Shape recovery of **CB5/silicone-silica** as a function of exposure time to 37°C water. [Color figure can be viewed in the online issue, which is available at wileyonlinelibrary.com.]

increase as water uptake increases due to the subsequent decrease in T_g (from ~71°C) which serves as the T_{trans} for shape recovery. Per Figure 8, specimens were fixed in a temporary U-shape geometry and recovery of the permanent linear geometry by exposure to 37°C water measured at designated time points. Prior to conditioning, all specimens exhibited no shape recovery (i.e., near perfect shape fixity). At 0.5 h, **SMP** already exhibited appreciable recovery, whereas the recovery was somewhat reduced for **CB5** and, particularly, for **CNT5**. In contrast, essentially no recovery was noted for composites coated with a silicone membrane. At 6 h, recovery for **SMP** was 12%, whereas that of **CB5** (9.4%) and **CNT5** (7.3%) was somewhat lower. The corresponding silicone coated composites displayed even lower recovery values with the lowest value observed for **CNT5/silicone$_{\text{-silica}}$** (4.3%). Notably, recovery was somewhat reduced for a given composite coated with a silica-filled silicone membrane versus an Al_2O_3-filled silicone. For these early stages of conditioning (≤6 h), the lack of appreciable shape recovery is consistent with the minimal depression of T_g depression due to a reduction in water absorption (Figure 4). At 24, 48, and 96 h, recovery increased substantially for all specimens with the highest observed for **SMP** (44.6, 89.2, and 99%, respectively) and the lowest for **CNT5/silicone$_{\text{-silica}}$** (17.4, 64.6, and 86.5%, respectively). Again, the extent of shape recovery coincides with the trends in water uptake and depression of T_g. For instance, at 96 h, recovery is quite significant (~87–99%) for all specimens. This coincides with the depression of the T_g values close to that of 37°C (Figure 4). By 192 h, all specimens displayed 100% recovery. Given the low thickness and relatively low modulus of the silicone membranes, mechanical interference by the membrane during shape recovery of coated SMP composites is believed to be negligible.

CONCLUSIONS

Towards realization of the biomedical utility of electroactive SMP composites capable of shape change via resistive heating, early shape recovery *in vivo* due to water uptake leading to T_g depression must be addressed. Towards this goal, we prepared SMP composites based on a thermoset PU matrix and CB and CNT fillers were coated with an Al_2O_3- or silica-filled silicone membrane to inhibit water diffusion. For the neat SMP (**SMP**) and SMP composites (**CB5** and **CNT5**), water uptake (37°C) and the subsequent depression of T_g (from ~71°C) was substantial during early periods of conditioning (≤6 h). In particular, the silica-filled silicone membrane, significantly reduced early stage water absorption. As conditioning continued to 192 h, the T_g values of all specimens, including coated composites, were decreased substantially due to water uptake and plasticization. The impact of T_g (i.e., T_{trans}) depression on the ability to fix the temporary shape was quantified by measuring shape recovery versus time conditioning in 37°C water. During early stages of conditioning (≤6 h), the silicone membranes (particularly the silica-filled silicone) diminished shape recovery. Subsequently, all specimens demonstrated a significant increase in shape recovery until reaching completion at 96–192 h. Thus, due to the ability to inhibit water absorption and T_g depression during early stages, silicone-coated electroactive SMP composite-based devices may afford the opportunity to facilitate controllable implantation (i.e., delivery and positioning within the body) by diminishing premature shape recovery prior to application of an electrical current. The retention of the "water-actuated" shape recovery in later stages may further facilitate maximum shape recovery, deployment and functionality of the device.

ACKNOWLEDGMENTS

This work was partially performed under the auspices of the U.S. Department of Energy by Lawrence Livermore National Laboratory under Contract DE-AC52-07NA27344 and supported by the National Institutes of Health/National Institute of Biomedical Imaging and Bioengineering Grant R01EB000462.

REFERENCES

1. Behl, M.; Lendlein, A. *Mater. Today* **2007**, *10*, 20.
2. Yang, B.; Min Huang, W.; Li, C.; Hoe Chor, J. *Eur. Polym. J.* **2005**, *41*, 1123.
3. Jung, Y. C.; Yoo, H. J.; Kim, Y. A.; Cho, J. W.; Endo, M. *Carbon* **2010**, *48*, 1598.
4. Gunes, I. S.; Jimenez, G. A.; Jana, S. C. *Carbon* **2009**, *47*, 981.
5. Gunes, I. S.; Cao, F.; Jana, S. C. *Polymer* **2008**, *49*, 2223.
6. Meng, Q.; Hu, J. *Compos. Part A: Appl. Sci. Manuf.* **2009**, *40*, 1661.
7. Rousseau, I. A. *Polym. Eng. Sci.* **2008**, *48*, 2075.
8. Leng, J. S.; Huang, W. M.; Lan, X.; Liu, Y. J.; Du, S. Y. *Appl. Phys. Lett.* **2008**, *92*, 204101.

9. Liu, Y.; Gall, K.; Dunn, M. L.; McCluskey, P. *Mech. Mater.* **2004**, *36*, 929.
10. Yakacki, C. M.; Satarkar, N. S.; Gall, K.; Likos, R.; Hilt, J. Z., *J. Appl. Polym. Sci.* **2009**, *112*, 3166.
11. Small, W. I.; Singhal, P.; Wilson, T. S.; Maitland, D. J. *J. Mater. Chem.* **2010**, *20*, 3356.
12. Sun, L.; Huang, W. M.; Ding, Z.; Zhao, Y.; Wang, C. C.; Purnawali, H.; Tang, C. *Mater. Des.* **2012**, *33*, 577.
13. Wilson, T. S.; Bearinger, J. P.; Herberg, J. L.; Marion, J. E.; Wright, W. J.; Evans, C. L.; Maitland, D. J. *J. Appl. Polym. Sci.* **2007**, *106*, 540.
14. Singhal, P.; Rodriguez, J. N.; Small, W.; Eagleston, S.; Van deWater, J.; Maitland, D. J.; Wilson, T. S. *J. Polym. Sci. Part B: Polym. Phys.* **2012**, *50*, 724.
15. Ortega, J.; Maitland, D.; Wilson, T.; Tsai, W.; Savaş, Ö.; Saloner, D. *Ann. Biomed. Eng.* **2007**, *35*, 1870.
16. Yang, B.; Huang, W. M.; Li, C.; Li, L. *Polymer* **2006**, *47*, 1348.
17. Sperling, L. H. Introduction to Physical Polymer Science; Wiley: Canada, **2001**.
18. Kim, B. Y. S.; Rutka, J. T.; Chan, W. C. W. *New Engl. J. Med.* **2010**, *363*, 2434.
19. Kim, S. J.; Lee, I. T.; Lee, H.-Y.; Kim, Y. H. *Smart Mater. Struct.* **2006**, *15*, 1540.
20. Zhuang, X.; Nikoozadeh, A.; Beasley, M. A.; Yaralioglu, G. G.; Khuri-Yakub B. T.; Pruitt B. L. *J. Micromech. Microeng.* **2007**, *17*, 994.
21. Sun, N.; Qin, S.; Wu, J.; Cong, C.; Qiao, Y.; Zhou, Q. *J. Nanosci. Nanotechnol.* **2012**, *12*, 7222.
22. Hawkins, M. L.; Grunlan, M. A. *J. Mater. Chem.* **2012**, *22*, 19540.
23. Rushton, D. N.; Brindley, G. S.; Polkey, C. E.; Browning, G. V. *J. Neurol. Neurosurg. Psychiatry* **1989**, *52*, 223.
24. Hron, P. *Polym. Int.* **2003**, *52*, 1531.
25. Bartzoka, V.; McDermott, M. R.; Brook, M. A. *Adv. Mater.* **1999**, *11*, 257.
26. Dyke, M. E. V.; Clarson, S. J.; Arshady, R. Silicone Biomaterials. An Introduction to Polymeric Biomaterials; Ed. Citus Books: London, **2003**.
27. Vondráček, P.; Doležel, B. *Biomaterials* **1984**, *5*, 209.
28. Curtis, J.; Colas, A. In Biomaterials Science; Ratner, B. D.; Hoffman, A. S.; Schoen, F. J.; Lemons, J. E., Eds.; Elsevier Academic Press: San Diego, CA, **2004**.
29. Kirkpartrick, S. *Rev. Modern Phys.* **1973**, *45*, 574.
30. Brinker, C. J.; Hurd, A. J.; Schunk, P. R.; Frye, G. C.; Ashley, C. S. *J. Non-crystalline Solids* **1992**, *147*, 424.
31. Zeng, J.; Saltysiak, B.; Johnson, W. S.; Schiraldi, D. A.; Kumar, S. *Compos. Part B: Eng.* **2004**, *35*, 173.
32. Dvornic, P. R. In Silicon-Containing Polymers: The Science and Technology of Their Synthesis and Applications; Jones, R. G.; Ando, W.; Chojnowski, J., Eds.; Kluwer Academic Publishers: Dordrecht, The Netherlands, **2000**.
33. Sangermano, M. B. R.; Malucelli, G.; Priola, A.; Pollicino, A.; Recca, A. *J. Appl. Polym. Sci.* **2003**, *89*, 1524.
34. Lau, K. K. S.; Bico, J.; Teo, K. B. K.; Chhowalla, M.; Amaratunga, G. A. J.; Milne, W. I.; McKinley, G. H.; Gleason, K. K. *Nano Lett.* **2003**, *3*, 1701.
35. Hong, Y. C.; Shin, D. H.; Cho, S. C.; Uhm, H. S. *Chem. Phys. Lett.* **2006**, *427*, 390.
36. Yang, B.; Huang, W. M.; Li, C.; Lee, C. M.; Li, L. *Smart Mater. Struct.* **2004**, *13*, 191.